

원자력 발전 원자로 용기의 열손실 설계인자에 관한 연구

김석범† · 박종호*

(원고접수일 : 2004년 5월 25일, 심사완료일 : 2004년 6월 22일)

Parametric Study on the Heat Loss of the Reactor Vessel in the Nuclear Power Plant

Seoug-Beom Kim† · Jong-Ho Park*

Abstract : The design parameter of the heat loss for the pressurized water reactor has been studied. The heat loss from the reactor vessel through the air gap, insulation are analysed by using the computational fluid dynamics code, FLUENT. Parametric study has been performed on the air gap width between the reactor vessel wall and the inner surface of the insulation, and on the insulation thickness. Also evaluated is the performance degradation due to the chimney effect due to gaps left between the panels during the installation of the insulation system. From the analysis results, the optimal width of air gap and insulation thickness and the value of heat loss are obtained. The results show how the heat loss varies with the air gap width and insulation thickness. The temperature and the velocity distributions are also presented. From the results of the evaluation, the optimal air gap width and the optimal insulation thickness are obtained. As the difference between the predicted heat loss and measured heat loss from the reactor vessel is construed primarily as losses due to chimney effect, the contribution of the chimney effect to the total heat loss is quantitatively indicated.

Key words : *Reactor coolant system, Reactor vessel insulation, Hot functional test, Chimney effect*

1. 서 론

The design parameter of the heat loss for the pressurized water reactor (1000 MWe) has been studied. The reactor coolant system (RCS) of the Yonggwang

Units 3 and 4 (YGN 3&4) in Korea consists of two identical heat transfer loops connected in parallel to the reactor vessel. Each loop contains one steam generator, two recirculating pumps and connecting pipe. A pressurizer is connected

† 책임저자(한국전력기술(주) 책임연구원), E-mail : green840@kornet.net, T : 042)868-4231

* 충남대학교 기계공학과 교수, E-mail : jhpark@cnu.ac.kr, T : 042)821-5645

to one of the reactor vessel outlet pipes. The design pressure and temperature of the RCS are 17.24MPa and 343.3°C^(1,2) respectively. The thermal insulation is provided for all components and pipes of the RCS. During the hot functional test of YGN 3, the measurements indicated that the RCS experienced an excessive heat loss. According to the report prepared by the Electric Power Research Institute⁽³⁾, most reactors show the excessive RCS heat loss of 2~3 times larger than the design heat loss during the plant heat loss test.

The Palo Verde Nuclear Generation Station (PVNGS, 1300 MWe) in the United States, which is the reference plant of the YGN 3 & 4, experienced the RCS heat loss of 3.62 MW during the heat loss test while the heat loss predicted by the design was 1.50 MW. The heat loss measurement using the infrared thermometry on each component was compared with the design heat loss. The ratio of the measured heat loss to the design heat loss was 0.0117/0.0293(MW to MW) for the pressurizer, 1.015/0.17 for two steam generators, and 0.491/0.064 for the reactor vessel excluding the control element driving mechanism, which indicated the 4~7 times large heat loss. The reflective insulation ($k=0.065$ W/m-°C⁽⁴⁾) which is made of thin stainless steel plates, is installed about 1.27~21.59cm apart from the reactor vessel allowing the air space to prevent the hot or cold spots on the vessel wall, to improve the insulation performance, and to avoid the chance of the chemical corrosion due to the dirt on the insulation. The insulation consists of the several panels, and each

panel is required to be tightened to its adjacent panels with the maximum allowable gap between each panel of 0.318cm^(1,2). When the external air flow enters the reflective panels, it contacts the vessel through the gap between the insulation and the vessel surface, the air is heated and rises to the top of the vessel, and eventually exits into the containment at high temperature. Such additional heat load, due to the transport of energy by the flow of air, may explain the excess heat loss from the vessel. The flow of infiltrated air is sustained by the pressure difference due to the temperature gradient, which can be termed 'chimney effect'^(1,2). The steam generator is the largest component in the containment building with the largest surface area and the largest number of insulation panels, i.e., with the largest potential for air infiltration area. Compared with the pressurizer, the steam generators operate at lower temperature, but they are of the considerably greater height. The survey in PVNGS determined a few vertical gaps up to 0.635cm and lap displaces by spaces up to 0.9525cm. The largest number of openings in the seams occurred in the horizontal seams with openings up to 2.54 cm. There are also many local openings with inadequate treatment for local air tightness. The reactor vessel operates differently from the other vessels such as a pressurizer or a steam generator in the fact that the cavity below the vessel is pressurized at 1.524cm^(1,2) of water, which can increase the infiltrating flow through the insulation gap. In this paper the heat loss from the reactor vessel has been analysed.

Parametric study has been performed

on the air gap width between the reactor vessel wall and the inner surface of the insulation, and on the insulation thickness. Also evaluated is the performance degradation due to the chimney effect due to the gaps left between the panels during the installation of the insulation system.

2. Governing equations

The heat transfer from the reactor vessel through the insulation is performed about analysis model, shown in Fig. 1 and 2. The air between the reactor vessel and the insulation is heated by the reactor surface and circulates due to the buoyancy force, and there occurs the heat loss through the insulation. The analysis handles the convective flow region and the conducting solid region of the insulation.

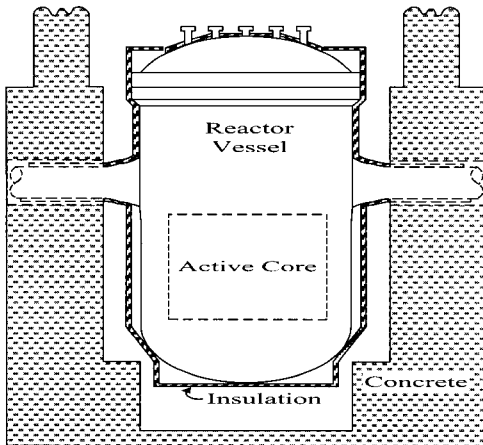


Fig. 1 Reactor vessel

The common approach in engineering analyses is to resolve the mean flow field, and to model the turbulent flow. The $k-\varepsilon$ turbulence model⁽⁵⁾, which is a widely

used model, has been utilized in the analysis. Here, k stands for the turbulent kinetic energy, and ε the dissipation rate.

In the momentum equation the Boussinesq approximation is used, which models the buoyancy force in terms of the temperature instead of the density variation. But the compressibility effects, viscous dissipation and radiation heat transfer of fluids are neglected according to evaluation results^(1,2).

The major assumptions to the steady state in 2-dimensional axis symmetry and the transfer to cylindrical coordinates which include the conservation of mass, continuity, Navier-Stokes of mean time, and energy equation are as follows:

Continuity equation

$$U \frac{\partial U}{\partial x} + V \frac{\partial V}{\partial r} + \frac{V}{r} = 0 \quad (1)$$

Axis momentum equation

$$U \frac{\partial U}{\partial x} + V \frac{\partial U}{\partial r} = -\frac{1}{\rho} \frac{\partial P}{\partial x} + \nu \left(\frac{\partial^2 U}{\partial x^2} + \frac{1}{r} \frac{\partial}{\partial r} \left(r \frac{\partial U}{\partial r} \right) - \frac{\partial (\overline{u^2})}{\partial x} - \frac{1}{r} \frac{\partial}{\partial r} (r \overline{uv}) \right) + g\beta(T - T_0) \quad (2)$$

Cylindrical momentum equation

$$U \frac{\partial V}{\partial x} + V \frac{\partial V}{\partial r} = -\frac{1}{\rho} \frac{\partial P}{\partial r} + \nu \left(\frac{\partial^2 V}{\partial x^2} + \frac{1}{r} \frac{\partial}{\partial r} \left(r \frac{\partial V}{\partial r} \right) - \frac{V}{r^2} \right) - \frac{1}{r} \frac{\partial}{\partial r} (r \overline{v^2}) - \frac{\partial (\overline{uv})}{\partial x} + \frac{\overline{w^2}}{r} \quad (3)$$

Energy equation

$$U \frac{\partial T}{\partial x} + V \frac{\partial T}{\partial r} = \frac{\partial}{\partial x} \left(a \frac{\partial T}{\partial x} - \overline{u\theta} \right) + \frac{1}{r} \frac{\partial}{\partial r} \left(r a \frac{\partial T}{\partial r} - r \overline{v\theta} \right) \quad (4)$$

The energy equation (4) is applied to turbulent flow of water, and due to the solid region with insulation has not velocity term as the following simplified expression.

$$0 = \frac{\partial}{\partial x} (\alpha_s \frac{\partial T}{\partial x}) + \frac{1}{r} \frac{\partial}{\partial r} (r \alpha_s \frac{\partial T}{\partial r}) \quad (5)$$

The Reynolds stresses are used this assumption as following model for eddy viscosity of Boussinesq.

$$-\overline{u_i u_j} = \nu_t (\frac{\partial U_i}{\partial x_j} + \frac{\partial U_j}{\partial x_i}) - \frac{2}{3} k \delta_{ij} \quad (6)$$

By the equation (6) rearranged as followings, respectively.

$$U \frac{\partial U}{\partial x} + V \frac{\partial U}{\partial r} = -\frac{1}{\rho} \frac{\partial P}{\partial x} + \frac{\partial}{\partial x} (\nu \frac{\partial U}{\partial x}) + \frac{1}{r} \frac{\partial}{\partial r} (r \nu \frac{\partial U}{\partial r}) + S_x \quad (7)$$

$$U \frac{\partial V}{\partial x} + V \frac{\partial V}{\partial r} = -\frac{1}{\rho} \frac{\partial P}{\partial r} + \frac{\partial}{\partial x} (\nu \frac{\partial V}{\partial x}) + \nu \frac{\partial}{\partial r} (r \nu \frac{\partial V}{\partial r}) + S_r \quad (8)$$

where,

$$S_x = \frac{\partial}{\partial x} (\nu_t \frac{\partial U}{\partial x}) + \frac{1}{r} \frac{\partial}{\partial r} (r \nu_t \frac{\partial V}{\partial x}) - \frac{2}{3} \frac{\partial k}{\partial x} + g \beta (T - T_0)$$

$$S_r = \frac{\partial}{\partial x} (\nu_t \frac{\partial U}{\partial r}) + \frac{1}{r} \frac{\partial}{\partial r} (r \nu_t \frac{\partial V}{\partial r}) - 2 \nu_t \frac{V}{r^2} - \frac{2}{3} \frac{\partial k}{\partial r}$$

The turbulent thermal diffusivity (α_t) is introduced as the required problem formulation. They are

$$\begin{aligned} -\overline{u\theta} &= \alpha_t \frac{\partial T}{\partial x} \\ -\overline{v\theta} &= \alpha_t \frac{\partial T}{\partial r} \end{aligned} \quad (9)$$

Numerical values for turbulence Prandtl numbers ($\sigma_t = \nu_t / \alpha_t$) with case of the internal flow have a range of 0.5 ~ 0.9 as researched by Reynolds⁽⁶⁾, Ludweig⁽⁷⁾, Johnson⁽⁸⁾. They are given to a value of 0.9. By substituting equation (9) into equation (4) the solution of conservation equation is obtained as follows:

$$\begin{aligned} U \frac{\partial T}{\partial x} + V \frac{\partial T}{\partial r} &= \frac{\partial}{\partial x} [(\frac{\nu}{\sigma} + \frac{\nu_t}{\sigma_t}) \frac{\partial T}{\partial x}] \\ &+ \frac{1}{r} \frac{\partial}{\partial r} [(\frac{\nu}{\sigma} + \frac{\nu_t}{\sigma_t}) r \frac{\partial T}{\partial r}] \end{aligned} \quad (10)$$

The velocity scale ($k^{1/2}$) and the length scale ($k^{3/2}/\epsilon$) are expressions defined to multiply form as following.

$$\nu_t = C_\mu \frac{k^2}{\epsilon} \quad (11)$$

Where C_μ is an empirically derived constant of proportionality. The values of k and ϵ required in equation (11) are obtained by solution of conservation equations.

$$\begin{aligned} U \frac{\partial k}{\partial x} + V \frac{\partial k}{\partial r} &= \frac{\partial}{\partial x} (\frac{\nu_t}{\sigma_k} \frac{\partial k}{\partial x}) \\ &+ \frac{1}{r} \frac{\partial}{\partial r} (\frac{\nu_t}{\sigma_k} r \frac{\partial k}{\partial r}) + P - \epsilon \end{aligned} \quad (12)$$

where,

$$\begin{aligned} U \frac{\partial \epsilon}{\partial x} + V \frac{\partial \epsilon}{\partial r} &= \frac{\partial}{\partial x} [\frac{\nu_t}{\sigma_\epsilon} \frac{\partial \epsilon}{\partial x}] \\ &+ \frac{1}{r} \frac{\partial}{\partial r} (\frac{\nu_t}{\sigma_\epsilon} r \frac{\partial \epsilon}{\partial r}) + C_{\epsilon 1} \frac{\epsilon}{k} P - C_{\epsilon 2} \frac{\epsilon^2}{k} \end{aligned} \quad (13)$$

$$\begin{aligned} P &= \nu_t \left[2 \left\{ \left(\frac{\partial U}{\partial x} \right)^2 + \left(\frac{\partial V}{\partial r} + \frac{V}{r} \right)^2 \right\} \right. \\ &\quad \left. + \left(\frac{\partial U}{\partial r} + \frac{\partial V}{\partial x} \right)^2 \right] \end{aligned} \quad (14)$$

Generally, numerical values for $C_{\epsilon 1}$, $C_{\epsilon 2}$, σ_k , and σ_ϵ are used in turbulence modeling.

They are given in Table 1.

Table 1 Values of k-ε model coefficients

C_{μ}	$C_{\epsilon 1}$	$C_{\epsilon 2}$	σ_k	σ_{ϵ}
0.09	1.44	1.92	1.0	1.3

The computational fluid dynamics code, FLUENT with SIMPLE algorithm⁽⁹⁾, has been used to evaluate the performance of the reflective insulation.

3. Numerical analysis

The reactor vessel, shown in Fig. 1, consists of the upper and lower dome head and the cylinder part. The control elements of the shutdown rods are located in the upper head area where the separate cooling system is provided. The lower head and the cylinder part are covered with the same insulation, but near the border region between the lower head and the cylinder part the air gap width between the reactor surface and the insulation is so narrow that the convection between each air space of the lower head and cylinder part can be neglected. In this analysis the cylinder part of the reactor is modeled and analysed, and Fig. 2 shows the analysis model. The radius, r_a , and the height, L , of the cylinder part are 226cm and 399cm, respectively. The air gap width and the insulation thickness vary depending upon the analysis cases. The air gap widths considered in the analyses are 1.27, 2.54, 5.08, 7.68, 10.16, 15.24, and 20.32cm, and the insulation thicknesses are 2.54, 5.08, 7.62, 11.43 and 15.24cm.

The temperature of the reactor surface

is assumed to be 295.8°C for all cases because the reactor control system controls the water temperature entering the reactor vessel to be maintained at 295.8°C.

The heat transfer coefficient of 5.68 W/m²·°C⁽¹⁰⁾ is applied to the outside surface of the insulation and the ambient temperature is assumed to be 35°C.

Several cases have been analysed to determine the sensitivity of the air gap size and the insulation thickness on the RCS heat loss. And to evaluate the 'chimney effect' on the heat loss, the opening between the insulation panels is turbulence modeled in the analysis. The pressure boundary condition with the difference of 0.00464 kg/cm^(1,2) on account of the elevation difference is imposed on at the lower and upper openings.

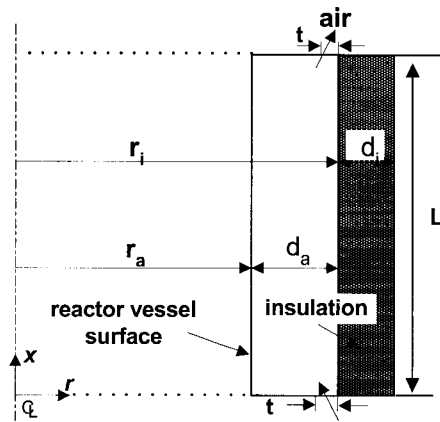


Fig. 2 Analysis model

Two cases with the opening sizes of 0.084 cm and 0.168cm are analyzed. Fig. 3 shows the boundary conditions. The computation is performed with the grid of 200x100, and the grid is concentrated near the openings.

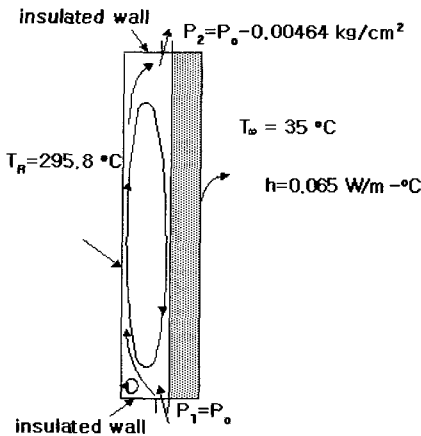


Fig. 3 Boundary condition.

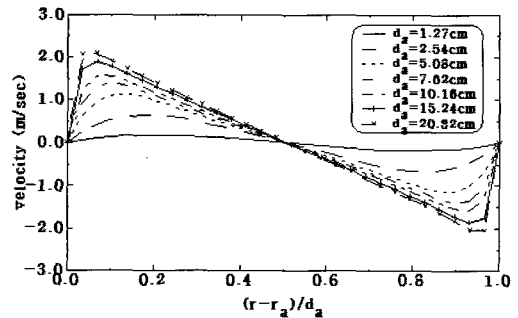
4. Results and discussions

4.1 Variation of the air gap width

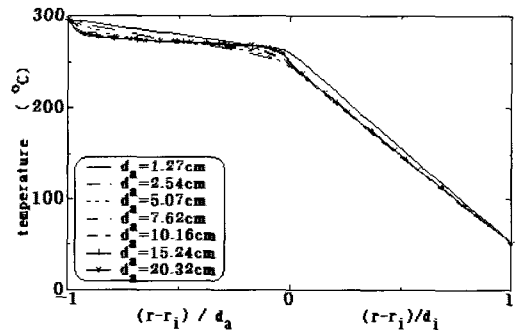
The heat transfer characteristics in accordance with the variation of the air gap width between the vessel wall and the insulation are considered with the insulation thickness of 11.43cm. Fig. 4 (a) shows that the convective air velocity increases as the gap width increases. When the gap is 1.27cm, the air is almost stagnant, and the temperature distribution across the gap at $x=L/2$ is linear, which indicates that the conduction heat transfer dominates (Fig. 4 (b)).

As the convection develops with the increase of the gap width, the temperature distributions at $x=L/2$ become similar. The highly convective recirculating flow is shown in the enclosure in case of the large air gap width. The effect of the convection becomes large in both ends of $x=0$ and $x=L$ with the increase of the gap. The temperature of the inner surface of the insulation varies in the whole region along the x -direction in case of the

gap of 20.32cm, while the end effect is limited in case of the narrower gap. The air between the vessel and the insulation is heated by the vessel surface while going up and is cooled by the insulation surface due to the heat loss while going down.



(a) Velocity distribution at $x/L=0.5$

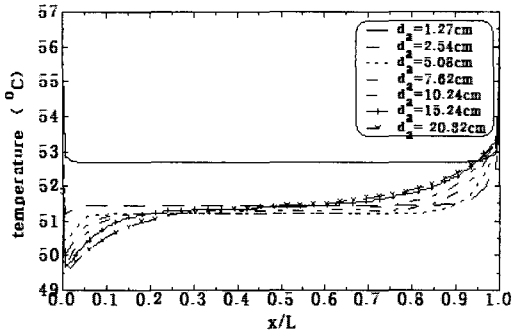


(b) Temperature distribution at $x/L=0.5$

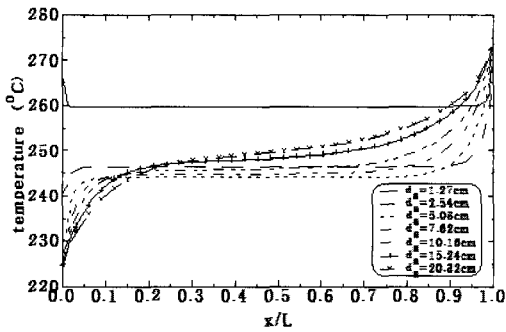
Fig. 4 Heat Transfer with variation of air gap width

The air temperature in the upper region is higher than the lower region, and the temperature distribution of the insulation surface is shown in Fig. 5, (a) and (b). The temperature of the insulation outer surface is lower than $60^{\circ}\text{C}^{(11)}$ in conformance with the insulation design requirement. Fig. 5, (c) shows that the heat flux from the vessel wall in the lower region becomes larger than that in the upper region as the gap increases. Since the

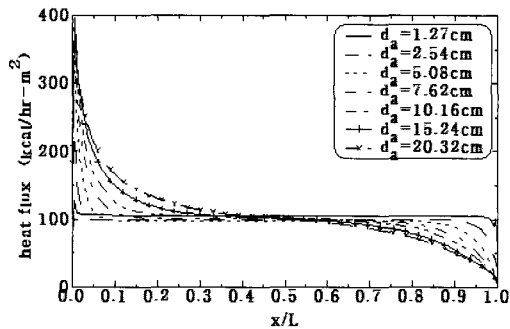
large differences in the temperature and heat flux of the lower and upper region are not desirable, these should be considered in the insulation design.



(a) Temperature distribution at insulation outer surface



(b) Temperature distribution at insulation inner surface

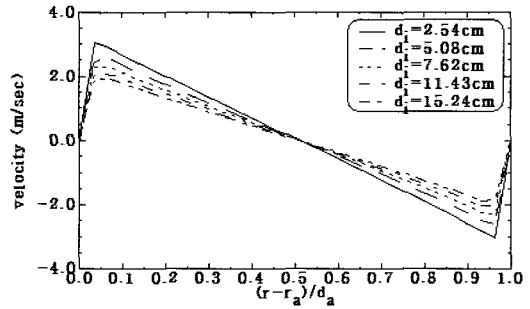


(c) Heat flux at the reactor surface

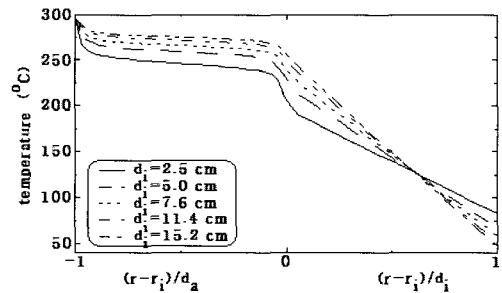
Fig. 5 Heat transfer with variation of air gap width

4.2 Variation of the insulation thickness

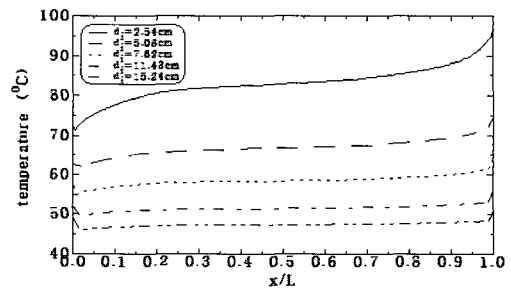
The heat transfer characteristics with the variation of the insulation thickness while the air gap is maintained at 20.32 cm. As the thickness of the insulation is decreased, the heat loss increases and the convection causes the wall temperature to vary along the wall surface.



(a) Velocity distribution at x/L



(b) Temperature distribution at x/L



(c) Temperature distribution at the insulation outer surface

Fig. 6 Heat transfer with variation of insulation thickness

The velocity and temperature distributions for the different insulation thicknesses are shown in Fig. 6, (a) and (b). Fig. 6, (c) indicates that the temperature of the outer surface of the insulation whose thickness is smaller than 5.08cm, exceeds the limit, 60°C required for the design, and in case of the thickness of 7.62cm the upper part of the insulation surface shows the higher temperature than 60°C.

The insulation thicker than 11.43cm, makes the outer surface temperature lower than 60°C. The heat loss with the insulation thickness of 2.54cm is about 2.5 times larger than that with 11.43cm.

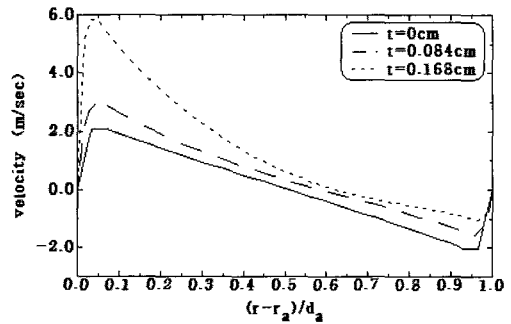
4.3 Consideration of the chimney effect

The heat loss due to the chimney effect is evaluated. The cold air infiltrating the insulation panels shows large effect on the heat transfer. As the convective air velocity is increased (Fig. 7, (a)), the air temperature between the reactor and the insulation is lowered by about 65.6°C compared with the case without the chimney effect (Fig. 7, (b)).

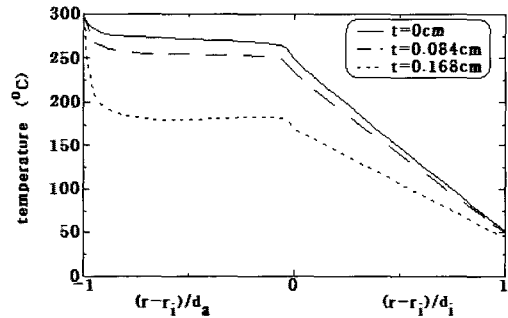
The chimney effect causes the heat flux from the reactor vessel to increase, especially in the lower part where the cold air infiltrates (Fig. 7, (c)). The dip in the heat flux distribution in the lower part is owing to the recirculating zone in the corner where the inlet air comes through the panel opening. In addition to the large heat loss, the infiltrating cold air can cause the undesirable cold spot on the reactor vessel.

The heat loss in each case is listed in Table 2. The heat loss in this case shows the minimum with the air gap width of

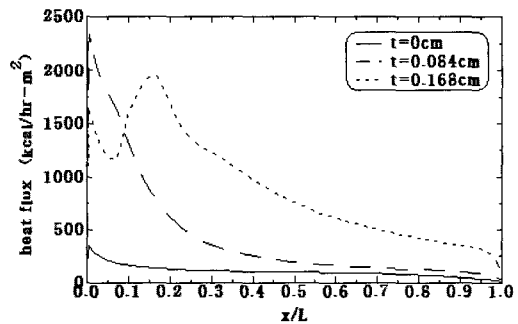
5.08cm and increases thereafter. Since the increase of the heat loss due to in the case of the opening size of 0.084cm and 8 times in the case of the opening size of 0.168cm, even a smaller opening between the insulation panels can have a serious impact on the design.



(a) Velocity distribution at x/L



(b) Temperature distribution at x/L



(c) Heat flux at the reactor surface

Fig. 7 Heat transfer with consideration of the chimney effect

The air entering the enclosure by the chimney effect exits at high temperature to the containment atmosphere, which degrades the efficiency of the reactor coolant system and causes the increase of the heat load to the HVAC of the containment building. Therefore, this heat load should be taken into account in determining the capacity of the HVAC.

Table 2 Comparison of the heat losses

(a) Variation of the air gap width	
air gap width (cm)	heat loss (kw)
1.27	1.103
2.54	1.042
5.08	1.033
7.62	1.062
10.16	1.093
15.24	1.108
20.32	1.131
(b) Variation of the insulation thickness	
insulation thickness(cm)	heat loss (kw)
2.54	2.840
5.08	1.961
7.62	1.486
11.43	1.131
15.24	0.923
(c) Consideration of the chimney effect	
opening size (cm)	heat loss (kw)
0.084	4.6
0.168	9.37

The reason why the heat losses in the tests of most plants are 2~3 times as much as the design values as in the EPRI report, is mainly because of the poor installation of insulation panels, not because of the defect of the insulation design itself. The insulation panel, therefore, should be carefully handled not to be damaged and the gap in the lap joints

between the panels should be maintained as small as possible.

Obviously, the corrective action is to close all openings to the maximum extent possible and to reduce the chimney effect by using horizontal convective seals. The 'chimney height' breakup by adding horizontal convective seals also effectively reduces the potential for air infiltration and exiting from the vessels.

The analysis shows that the poor installation and the panel damage due to the improper storage or handling cause non-design gaps in the lap joints between the panels and lead to the serious degradation of the system performance due to chimney effect. The data from this study can be used for the insulation design of the large equipment in various plants

5. Conclusions

A numerical study is performed to optimize the insulation design and to investigate the chimney effect due to poor installation of the insulation panels. From the results of this study, it is concluded that:

The air gap width between the reactor wall and insulation minimizing the heat loss is 5.08cm. In order to maintain the outer surface temperature of the insulation below 60°C, the insulation thickness of 11.43cm is adequate. Since the heat loss is increased eight times even with a half of the allowed opening size, the opening between the insulation panels should be kept as small as possible, and the horizontal convective seals in order to reduce the chimney effect should be used.

References

- [1] Mahlmeister, J.: Evaluation of Heat Loss to Containment from the Reactor Coolant System, PVNGS, Study No. 13-MS-31, Rev. 1 Oct. 1984
- [2] Mahlmeister, J.: Evaluation of Heat Loss to Containment from the Reactor Coolant System, PVNGS, Sep. 1983
- [3] Palo Alto, Electric Power Research Institute, Chp. 3, Volume II, Reactor Coolant System and Reactor Non-Safety Aux. Sys., 1983
- [4] Edward J.: Wolbert, Transco Products inc., Analytical Thermal Report, July, 1, 1991
- [5] FLUENT Version 6.1, Fluent Inc., Lebanon, New Hampshire. (2003)
- [6] Reynolds, W. C. Kays, and Kline S.J.: Heat Transfer in the Turbulent Incompressible Boundary Layer. I. Constant Wall Temperature. NASA Memo. 12-1-58 W, 1958; II. Step Wall Temperature Distribution. NASA Memo. 12-2-58W, 1958 ; III. Arbitrary Wall Temperature and flux. NASA Memo. 12-3-58W(1958) ; IV. Effect of Location of Transition and Prediction of Heat Transfer in a Known Transition Region. NASA Memo.12-58W, 1958.
- [7] Ludwig, H.: Bestimmung des erhaeltnisses der Austausch Koeffizienten Fuer Waerme und Impuls bei Turbulenten Grenzschi-chten, ZFW 4,73-81, 1956.
- [8] Johnson, D.S: Velocity and Temperature Fluctuation Measurements in a Turbulent Boundary Layer Downstream of Stepwise Discontinuity in Wall Temperature, Trans. ASME J. Appl. Mech. 26, 325-336, 1959.
- [9] Patanker, S.V.: Numerical Heat Transfer and Fluid Flow, McGRAW-HILL, 1980.1.
- [10] Leschziner, M. A. and Rodi W.: Calculation of Annular and Twin Parallel Jets using Various Discretization Schemes and Turbulence Model Variations, ASME J. of Fluid, Eng., Vol. 103, pp. 352-360, 1981.
- [11] McChesney, M. and McChesney, P.: Feul Save Associates, Preventing Burns from Insulated Pipe, July 1981

저 자 소 개



김석범 (金錫範)

1963년 출생, 1998년 충남대학교 기계공학(석사), 2004년 충남대학교 기계공학(박사학위 수료), 1989년 삼성전자(정보통신분야)연구원, 1990년 한국원자력연구소(연구원), 1998. 11~ 현재 한국전력기술(주) 책임연구원



박종호 (朴鍾鎬)

1951년 출생, 1973년 전북대학교 공과대학 기계공학과(학사), 1975년 전북대학교 대학원 기계공학전공(석사), 1985년 전북대학교 대학원, 기계공학전공(박사), 1976-1978년 충남대학교 공과대학 정밀기계공학조교, 1978. 6-2004 현재 충남대 공과대학 기계공학과 전임강사~교수, 관심분야: 초음속 및 아음속 유동 열음향 냉동기·유체기계